Journal of Electroceramics 5:1, 53–61, 2000

$(Ba,Ca)TiO_3$ PTCR Ceramics with $LaNiO_3$ Thin-Film Electrodes: Preparation and Characterization of the Interface

BERND TRUMMER,[1] OTTO FRUHWIRTH,[1] KLAUS REICHMANN,[1] GERHARD HERZOG,[1]
WERNER SITTE[2] & MICHAEL HOLZINGER[2]

[1]*Institut für Chemische Technologie anorganischer Stoffe, TU-Graz, Stremayrgasse 16/III, A-8010 Graz*
[2]*Institut für Physikalische und Theoretische Chemie, TU-Graz, Technikerstraße 4/I, A-8010 Graz*

Submitted April 9, 1999; Revised February 14, 2000; Accepted February 23, 2000

Abstract. Conductive $LaNiO_3$ thin film electrodes were deposited by chemical solution deposition (CSD) from nitrate solutions onto polycrystalline Al_2O_3 and $(Ba,Ca)TiO_3$ PTCR ceramic substrates. The electrical properties of the $LaNiO_3$ thin film on Al_2O_3 and of the interface consisting of $LaNiO_3$ and the semiconductive oxide ceramic were investigated. The deposited $LaNiO_3$ films were about 250 nm thick and consisted of nanosized particles. The resistivity of the $LaNiO_3$ film was about 3×10^{-3} Ωcm at 20°C. The PTCR ceramic consisted of μm sized particles and exhibited an electronic resistivity of about 10 Ωcm at 20°C and a steep increase of the resistivity of a few orders of magnitude above the Curie point at about 120°C. The electrical properties of the $LaNiO_3$/PTCR interface were dominated by the properties of a barrier layer between the PTCR ceramic and the $LaNiO_3$ electrode. The potential dependence of the impedance indicated that the barrier layer consisted of a depletion layer within the PTCR ceramic, when the flat band potential of $LaNiO_3$ on the PTCR ceramic at about -250 mV was exceeded. Additionally the formation of an insulating layer at the $LaNiO_3$ electrode has to be taken into account.

Keywords: PTCR, conducting perovskites, interface, barrier layer, mott-schottky theory

1. Introduction

Perovskite oxide ceramics exhibit a wide range of physical properties such as conductivity, ferroelectricity, giant magnetoresistance or even catalytic activity [1,2]. One of the most interesting perovskite oxides is $BaTiO_3$, which is applied commercially as dielectric material in ceramic capacitors. The addition of small amounts of donor dopants (e.g., Y^{3+}, La^{3+} for Ba^{2+} or Sb^{5+} for Ti^{4+}) transforms the highly insulating $BaTiO_3$ into an n-type conducting oxide with an appreciably low resistivity of about 10 Ωcm [3] at room temperature and a large positive temperature coefficient of resistivity (PTCR) towards higher temperatures [4]. The addition of small amounts of acceptor dopants (e.g., Mn^{3+} for Ti^{4+}) results in increasing resistivities, but does not show any discernable influence on the PTCR effect as long as the concentration of the acceptor dopants remains several orders of magnitude smaller than the concentration of the donor dopants [5].

For their usual application, PTCR ceramics have to be connected barrier free (i.e., ohmic) to electrodes, which can imply serious problems with a large number of materials. Since PTCR ceramics are semiconductors, electronic or ionic charge carrier interactions between the PTCR ceramic and the electrode material may take place. This behavior is known for many metallic electrodes (e.g., Cu, Ag) which cause large barrier layers, partly related to the formation of depletion layers in the semiconductor, partly related to the formation of insulating layers between semiconductor and electrode. Only a small number of base metals (e.g., In, Ga, Zn) yields barrier

free contacts to the PTCR ceramic. So far, only little attention has been paid to the behavior of electrodes consisting of conductive oxides. Conductive oxides of the perovskite family are promising candidates for substituting metal electrodes on PTCR ceramics. For several conductive perovskite oxides like $YBa_2Cu_3O_{6+x}$ (YBCO) [6], $LaNi_{1-x}Co_xO_3$ [7] and $La_{0.8}Sr_{0.2}CoO_3$ [8] it has been demonstrated that they are well suited as electrodes in electronic devices such as negative temperature coefficient resistors (NTCRs) [9] or ferroelectric substrates [10] due to the significant improvement on the aging of the NTCR-sensors and on the fatigue of ferroelectric memories. In general, perovskite oxides are both chemically and crystallographically compatible with perovskite oxide substrates. Regarding the preparation of perovskite oxide electrodes, different techniques are available. Conventional co-sintering results in thick films, laser ablation [11], sputtering [12], sol-gel deposition [13,14] and chemical solution deposition (CSD) [15] allows to produce thin films. Thickness, composition and electrical properties strongly depend on the deposition method.

From the large number of perovskite oxides with high conductivity $LaNiO_3$ is one of the most promising materials for electrode purposes. $LaNiO_3$ is reported to be a metallic oxide [16,17] with room temperature resistivities between 1.6×10^{-3} and 6.6×10^{-2} Ωcm^{-1}, depending on the preparation conditions [18,19]. It crystallizes in a rhombohedrally distorted perovskite structure. Since $LaNiO_3$ is thermally not stable in air above 860°C [20], $LaNiO_3$ electrodes cannot be prepared by co-sintering of $LaNiO_3$ and $BaTiO_3$ ceramics, a process which requires a sintering temperature up to 1400°C. Moreover ion-interdiffusion would destroy the PTCR effect. Alternatively, Li et al. [21] report the formation of $LaNiO_3$ thin-films with metallic conductivity by thermal decomposition of metalorganic compounds at temperatures as low as 550°C on single crystals of Si and quartz.

In this paper we will report about the growth of $LaNiO_3$ thin film electrodes on polycrystalline Al_2O_3 and on polycrystalline donor doped (Ba,Ca)TiO_3 PTCR ceramics. The electrodes were obtained by CSD of nitrate precursors. The electrical properties of the ceramics will be characterized and a description of the properties of the $LaNiO_3$/PTCR interface, compared with the properties of PTCR ceramics with Ag and with InGa electrodes, will be given. Subsequently, we will apply a model based on the Mott-Schottky theory to explain the electrical properties of the interface.

2. Experimental

For the preparation of $LaNiO_3$ films by CSD $La(NO_3)_3 \cdot 6\ H_2O$ and $Ni(NO_3)_2 \cdot 6\ H_2O$ were dissolved in stoichiometric ratio (1 : 1) in a mixture of ethanol/buthylacetate (1 : 4) to yield 0.25 molar solutions. Sintered Al_2O_3 plates and semiconducting PTCR pellets were coated with $LaNiO_3$ thin films. The $LaNiO_3$ on Al_2O_3 allowed the characterizing of the electrical properties of the $LaNiO_3$ film itself, the $LaNiO_3$/PTCR-combination the characterizing of the electrical behavior of the interface.

Film deposition was performed by a spin coating technique at 4000 rpm for 60 s. After deposition the samples were heated rapidly in air to 530°C and to pyrolysize for 60 min. The respective film thickness was obtained by three times repeating the deposition/pyrolysis process. In a final step the samples were annealed in air at 790°C for 2 h. Phase identification was carried out by grazing incidence X-ray diffraction (Siemens D5005), composition, morphology and thickness of the layers were investigated by scanning electron microscopy with EDX-analysis (Leo 982 Gemini). Temperature dependent dc-conductivities of the $LaNiO_3$ were obtained using the van der Pauw-technique, which cancels out the contact resistances of the measuring electrodes. For this purpose four silver paint dots were deposited as contacts at the periphery of the disk shaped samples.

The investigated PTCR-ceramics (pellets of 5 mm diameter and 1 mm thickness, supplied by Siemens + Matsushita Components) consisted of $(Ba_{0.75}Ca_{0.25})TiO_3$, doped with Y and Mn. The specimens were n-conducting with a resistivity of about 10 Ωcm at room temperature. The Curie temperature was determined by DSC (Netzsch STA 409) with an onset temperature of 116.7°C. As base metal contacts, AgZn electrodes (Gwent Electronic Materials), fired at 570°C, were compared with InGa electrodes, which were rubbed onto the PTCR ceramics at room temperature. Both electrode materials yielded ohmic contacts. Because of better handling AgZn was used as bottom electrode in all samples. The specimens for the electrical measure-

ment consisted of a PTCR-pellet with AgZn as bottom electrode and the test electrode ($LaNiO_3$ or Ag) as top electrode. The Ag electrodes were fired onto the PTCR pellet at 700°C for 30 min. The $LaNiO_3$ electrode was additionally covered with AgZn in order to avoid contact resistances between the oxide electrode and the sample holder (gold plated clamps).

Total resistances of these $LaNiO_3$/PTCR- and Ag/PTCR-combinations were measured conventionally using a Wenking LT-78 galvanostat and a Knick voltmeter. The ac properties of the ceramics including the bias dependence were studied with a Hewlett Packard 4192A impedance analyzer, operating within a frequency range from 5 Hz to 13 MHz at a voltage amplitude of 30 mV. For biased measurements the AgZn bottom electrode served as potential reference (ground) and the test electrode ($LaNiO_3$ or Ag) was polarized positively or negatively with respect to ground.

3. Results

Spin-coating of the respective nitrates and subsequent thermal decomposition resulted in dense, smooth and crack-free thin films of polycrystalline, single phase $LaNiO_3$ on polycrystalline Al_2O_3 and on polycrystalline PTCR substrates (Fig. 1). The $LaNiO_3$ thin film consisted of particles of 50–100 nm size (Fig. 2). The deposition of three layers before annealing resulted in 250 nm thick $LaNiO_3$ films. The PTCR-ceramic consisted of μm-sized particles.

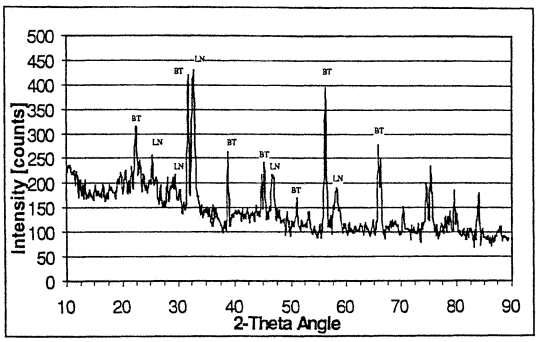

Fig. 1. XRD pattern of $LaNiO_3$ (LN) on a polycrystalline PTCR substrate (BT).

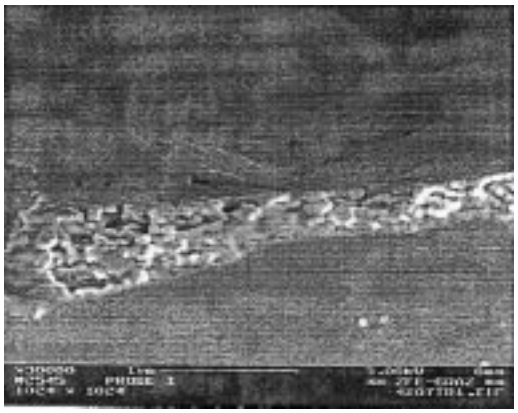

Fig. 2. SEM micrograph of a $LaNiO_3$ film on a polycrystalline Al_2O_3 substrate. View on the edge of the fractured sample.

3.1. *Electrical Properties*

The dc resistivity of the $LaNiO_3$ films on Al_2O_3 was about 3×10^{-3} Ωcm at 20°C and increased slightly with temperature (Fig. 3). The resistivity of the PTCR ceramic amounted to approximately 10 Ωcm at 20°C and showed an increase of a few orders of magnitude at the Curie point at about 120°C. The choice of different electrodes significantly influenced the temperature dependence of the resistance (Fig. 4). InGa and AgZn electrodes showed small resistances between room temperature and the Curie point and a steep increase of the resistance of about 3 orders of magnitude above the Curie point. This kind of behavior can be expected for barrier free contacts between an electrode and the PTCR-ceramic. PTCR-ceramics with $LaNiO_3$ and Ag electrodes exhibited larger resistances between room temperature and the

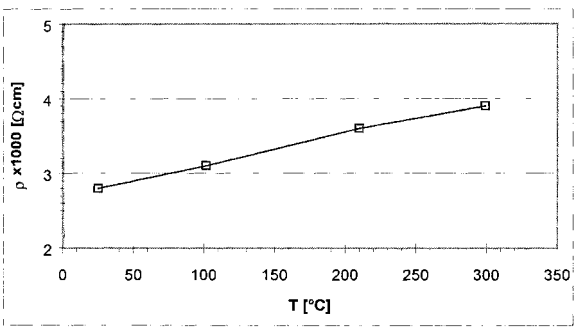

Fig. 3. Temperature dependence of the dc resistivity of a $LaNiO_3$ film on a polycrystalline Al_2O_3 substrate.

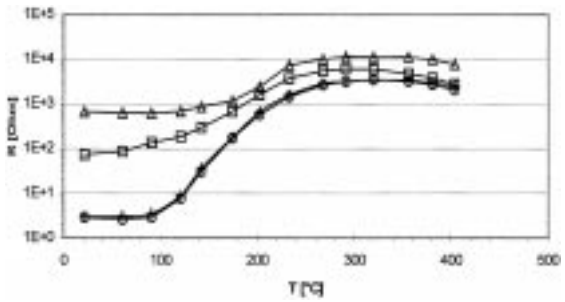

Fig. 4. Temperature dependence of the resistance (dc) of a PTCR pellet with different electrode materials (-○- In/Ga, -+- Ag/Zn, -△- Ag, -□- $LaNiO_3$).

Curie point reaching approximately the same resistance above the Curie point. The increase of the total resistance at room temperature (InGa/PTCR = 3 Ω, $LaNiO_3$/PTCR = 80 Ω, Ag/PTCR = 800 Ω) was correlated with a decrease of the total change of the resistance above the Curie point from three orders of magnitude for InGa/PTCR to two orders of magnitude for $LaNiO_3$ and one order of magnitude for Ag/PTCR.

The ac behavior of different interfaces was studied by separating the complex impedance into its real part (expressed as resistance R_p) and into its imaginary part (expressed as parallel capacitance C_p). PTCR ceramics with InGa or AgZn electrodes exhibited ohmic contacts with small and constant values of R_p and C_p over the frequency range investigated. Contrary to InGa/PTCR- and AgZn/PTCR-interfaces, the $LaNiO_3$/PTCR- and Ag/PTCR-interfaces showed strong frequency dependencies of the resistance and the capacitance (Figs. 5 and 6). In the low frequency

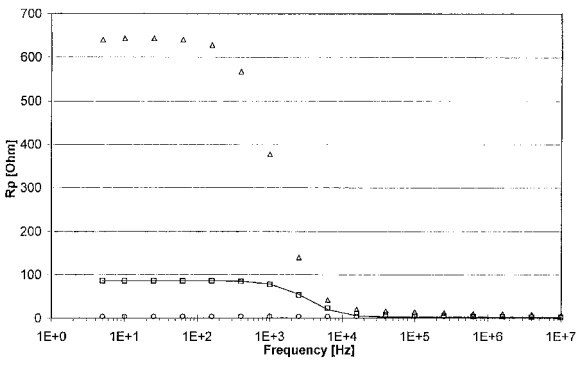

Fig. 5. Frequency dependence of the resistance R_p at room temperature of the PTCR ceramics with different electrode materials (○ In/Ga, △ Ag, □ $LaNiO_3$, — equivalent circuit calculations for $LaNiO_3$/PTCR).

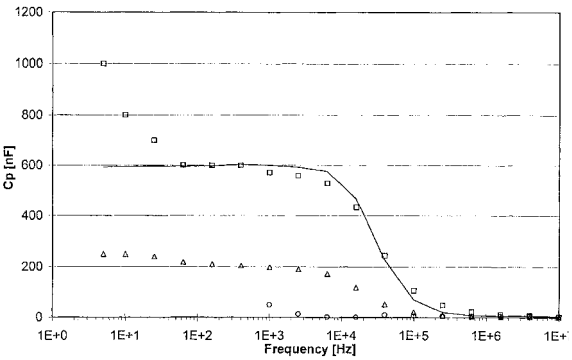

Fig. 6. Frequency dependence of the capacitance C_p at room temperature of the PTCR ceramics with different electrode materials (○ In/Ga, △ Ag, □ $LaNiO_3$, — equivalent circuit calculations for $LaNiO_3$/PTCR).

range the ac and dc resistances were almost identical. The resistance of the Ag/PTCR-interface was generally larger compared to the $LaNiO_3$/PTCR interface. With increasing frequencies R_p decreased for one order of magnitude in the case of $LaNiO_3$ and two orders of magnitude in the case of Ag electrodes. In the high frequency range both combinations approached small resistances similar to the InGa/PTCR interface. A similar frequency dependence was observed for the capacitances of the $LaNiO_3$/PTCR- and the Ag/PTCR-interfaces. The low frequency range was characterized by large and almost constant capacitances, which decreased by about 2 orders of magnitude towards higher frequencies. The capacitances of the $LaNiO_3$/PTCR interface were larger than the capacitances of the Ag/PTCR-interface. For both interfaces the high frequency range was characterized by small and constant capacitances which were similar to those of the InGa/PTCR-interface.

In addition to the frequency dependencies, the resistances and capacitances of the $LaNiO_3$/PTCR- and the Ag/PTCR-interface also exhibited a pronounced dependence on the applied bias voltage (Figs. 7 and 8). It should be noted again, that one side of the PTCR pellet was performed with an AgZn electrode, which served as potential reference (ground). The other side gained the test electrodes ($LaNiO_3$ or Ag; working electrode), which were polarized positively or negatively. Both the $LaNiO_3$/PTCR- and the Ag/PTCR-interface showed a maximum of R_p at 0 V bias voltage. Towards increasing potentials R_p decreased rapidly and reached constant, but different values for positive and negative

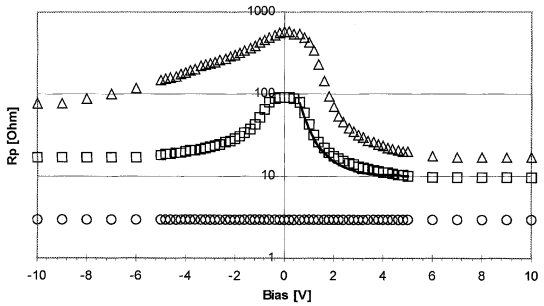

Fig. 7. Influence of the applied bias voltage on the resistance R_p at 1 kHz and room temperature of the PTCR ceramics with different electrode materials (○ In/Ga, △ Ag, □ $LaNiO_3$, — calculated data). The sign of the bias voltage refers to the voltage on the test electrode.

potentials. Also the capacitances of the $LaNiO_3$/PTCR- and the Ag/PTCR-interfaces showed significant dependencies on the applied bias voltage. $LaNiO_3$/PTCR-interfaces exhibited large capacitances at low voltages, which disappeared rapidly and almost symmetrically towards increasing positive or negative potentials. At high potentials constant capacitances were approached but small differences between positive and negative potentials remained. A shallow maximum was found at about 1.5 V for the Ag/PTCR-interface and the capacitances were smaller than those of the $LaNiO_3$/PTCR-interface (Fig. 8) with a pronounced asymmetry. For $LaNiO_3$/PTCR- and Ag/PTCR-interfaces increasing negative potentials resulted in a slow decrease of the capacitance, whereas towards positive potentials a considerable decrease of the capacitance was observed. Constant capacitances with different amounts for positive and

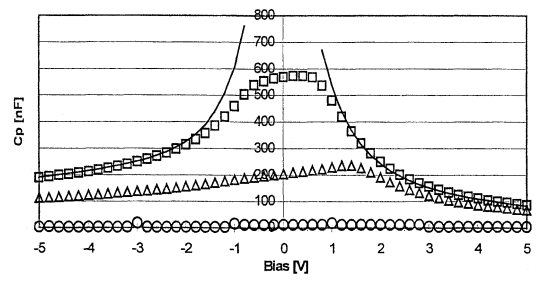

Fig. 8. Influence of the applied bias voltage on the capacitance C_p at 1 kHz and room temperature of the PTCR ceramics with different electrode materials (○ In/Ga, △ Ag, □ $LaNiO_3$, — calculated data). The sign of the bias voltage refers to the voltage on the test electrode.

negative potentials were approached at high potentials. Contrary to Ag and $LaNiO_3$ electrodes, InGa did not show any bias dependence.

4. Discussion

$LaNiO_3$ thin films derived from nitrate precursors exhibited resistivities of about the same amount as $LaNiO_3$ thin films derived from metal-alkylates [21]. In comparison to metal alkylates, the deposition of $LaNiO_3$ films from nitrates requires little effort in preparation and offers a comfortable and fast route.

The investigation of the electrical properties of the ceramic samples revealed that the specific resistivity of the $LaNiO_3$ film is significantly smaller than that of the PTCR substrate. To a first approximation one could assume that the electrical properties of the interface are dominated by the ceramic with the larger resistivity (as with two different resistances in series) and therefore the interface to be influenced mainly by the properties of the PTCR ceramic.

A comparison of the dc and ac properties of the $LaNiO_3$/PTCR-interface and the PTCR ceramic with metal electrodes revealed that the properties of the $LaNiO_3$/PTCR-interface can be placed between the behavior of PTCR ceramics with base metal electrodes exhibiting ohmic contacts (AgZn, InGa) and PTCR ceramics with noble metal electrodes, which show more or less pronounced barrier layers. Therefore, we used a theoretical approach similar to metal/semiconductor junctions for the explanation of the processes that take place at the $LaNiO_3$/PTCR interface.

The occurrence of high resistances between metals and semiconductors is generally explained by the formation of barrier layers due to electronic or chemical reasons. Very often, the formation of a depletion layer within the semiconductor is assumed, which can be expected, if the Fermi-level of the electrode material is lower than the Fermi level of the semiconductor. This is generally the case for noble metal electrodes. The formation of depletion layers is attributed to the adaptation of the different Fermi-levels, which requires an electron transfer from the semiconductor to the metal surface and results in the formation of a space charge region. A quantitative description of this behavior can be given by the Mott-Schottky theory. Another possibility of introducing high resistances is the occurrence of surface reactions

between the electrode and the semiconductor during the deposition of the electrodes. This may result in the formation of insulating layers between the metal and the semiconductor.

4.1. Modeling the Electrical Behavior of the $LaNiO_3$/PTCR Ceramic Interface

Impedance spectroscopy of the $LaNiO_3$/PTCR interface revealed a strong frequency dependence of the impedance, but showed constant values in the low and high frequency regime. A comparison of the $LaNiO_3$/PTCR-interface with the barrier-free InGa/PTCR-interface revealed an almost identical behavior in the high frequency range, thereby indicating the dominance of the PTCR ceramic on the electrical properties at high frequencies. Consequently, the differences of the electrical behavior in the low frequency range were attributed to the properties of the barrier layer.

Based on these assumptions the $LaNiO_3$/PTCR-interface was modeled by an equivalent circuit consisting of two RC-elements in series for the PTCR ceramic and the barrier layer (Fig. 9). The frequency dependence of the impedance as fitted to this model resulted in capacitances of 2.2 nF for the PTCR ceramic and 580 nF for the barrier layer and resistances of 3 Ω for the PTCR ceramic and 84 Ω for the barrier layer. The resistivity of the bulk $LaNiO_3$ layer was very small and thus negligible for the behavior of the entire interface. Calculations of the capacitances and the resistances based upon these assumptions were in good agreement with experimental data (Figs. 5 and 6). The large capacitance of the PTCR ceramic were attributed to its internal grain boundaries [10,22].

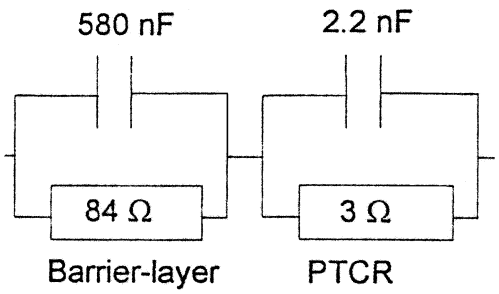

Fig. 9. Equivalent circuit for modeling of the $LaNiO_3$/PTCR interface.

4.2. Characterizing the Barrier Layer

A more detailed insight into the physical processes that are involved in the formation of the barrier layer was available from the potential dependence of the impedance of the $LaNiO_3$/PTCR-interface. This investigation was carried out at a frequency of 1 kHz, where the electrical properties of the $LaNiO_3$/PTCR interface were dominated by the properties of the barrier layer (Figs. 5 and 6). The potential dependence of the impedance (Figs. 7 and 8) exhibited small but significant differences between potentials of the same magnitude but of opposite signs thus making it necessary to distinguish between forward and reversed bias conditions. Qualitatively the same behavior is observed with the Ag/PTCR-interface. Experimental data obtained under reversed bias conditions can be interpreted assuming a depletion layer. On the other hand, for forward bias condition a different mechanism for the formation of a barrier layer has to be considered.

Forward bias conditions were observed when the test electrode ($LaNiO_3$ or Ag) was connected to positive potentials with respect to the grounded PTCR/AgZn back side. At high potentials (positive or negative) R_p approached constant values (Fig. 7). The resistance R_p of the interface exhibited a maximum at 0 V and decreased proportional to the applied potential φ according to

$$R_p \propto \frac{1}{\varphi \exp(2.9/-\varphi)} \tag{1}$$

No significant temperature dependence of the resistance was observed in the temperature range between 20°C and 100°C. The exponential factor of 2.9 eV in Eq. (1) was taken from [23] and represents the band gap energy of La-doped $BaTiO_3$ PTCR ceramics. Eq. (1) describes the potential dependence of the resistance of thin insulating films in between a metal and a semiconductor, which is characterized by a sharp decrease of resistivity above a certain potential limit caused by Fowler-Nordheim tunneling. Fowler-Nordheim tunneling is limited to insulating layers with a thickness less than 10 nm [24]. Measured and calculated data are compared in Figs. 7 and 8 (right branch, positive potentials).

The investigation of the potential dependence of the capacitance of the $LaNiO_3$/PTCR-interface revealed constant capacitances for small positive

potentials and a decrease of the capacitances proportional to $1/\varphi$ for potentials exceeding $+1\,V$ (Fig. 8, right branch). This behavior is similar to a plate capacitor with a constant distance between the plates. Similar potential dependencies of R_p and C_p were observed also for Ag/PTCR-interfaces (Figs. 7, 8), therefore the formation of an insulating layer has to be considered for this case too.

Reversed bias conditions were observed when the test electrode was connected to negative potentials. Resistances from reversed bias conditions were slightly larger than resistances from forward bias conditions, thus making it necessary to introduce an additional resistance to explain the properties of the $LaNiO_3$/PTCR-interface.

The capacitance of the $LaNiO_3$/PTCR-interface revealed a potential dependence similar to the behavior of semiconductors with depletion layers (Fig. 8, left branch). Dewald [25] demonstrated for n-doped semiconducting ZnO ceramics that the capacitance of such a space charge is proportional to the reciprocal of the square root of the potential decrease in the depletion layer as

$$\frac{1}{C^2_{sc}} = \frac{2}{\varepsilon_0 \varepsilon_{sc} e n_0}(-\varphi_{sc}) - \frac{kT}{e} \tag{2}$$

C_{sc} is the space charge capacitance, φ_{sc} the potential decrease in the depletion layer, ε_0 the dielectric permittivity of the vacuum, ε_{sc} the permittivity of the space-charge region, n_0 the number of ionized donor atoms, k the Boltzmann factor, T the absolute temperature and e the electron charge.

Equation (2), generally called Mott-Schottky approximation, is valid for positive potentials only. A Mott-Schottky plot of the capacitances of the $LaNiO_3$/PTCR and the Ag/PTCR interface enables us to localize the depletion layer within the PTCR ceramic (Fig. 10). An extrapolation of $1/C^2 \rightarrow 0$, corrected by the term kT/e reveals a flat band potential φ_0 of $-225\,mV$ for the $LaNiO_3$/PTCR interface and a flat band potential of $+1.5\,V$ for the Ag/PTCR interface.

The depth of the space charge within the PTCR ceramic can be estimated from the slope of the linear part of the Mott-Schottky plot which primarily yields the number of ionized donor atoms n_0 within the PTCR ceramic.

The Debye-length L_D is correlated to n_0 and can be calculated from [26]

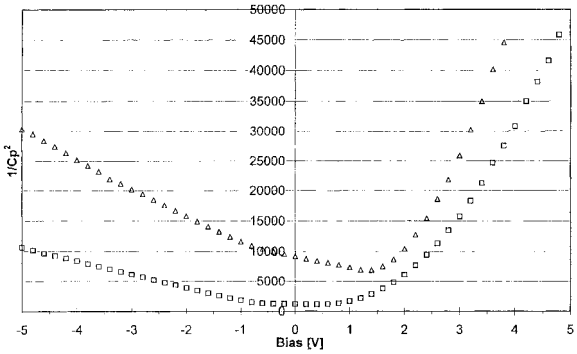

Fig. 10. Mott-Schottky plot of the capacitance Cp at 1 kHz and room temperature for the $LaNiO_3$/PTCR interface (□) and the Ag/PTCR interface (△). The sign of the bias voltage refers to the voltage on the test electrode.

$$L_D = \sqrt{\frac{\varepsilon_0 \varepsilon_{sc} kT}{e^2 n_0}} \tag{3}$$

The depth d of the depletion layer in the semiconductor is a function of the Debye-length L_D, the flat band potential φ_0 and the temperature T according to

$$d = L_D \sqrt{\frac{2e|\varphi_0|}{kT}} \tag{4}$$

From these calculations depletion layer thicknesses of $0.63\,\mu m$ for $LaNiO_3$ and $2.1\,\mu m$ for Ag electrodes were obtained for 20°C.

According to [27] the number of surface states N_{SS} at the interface can be calculated starting from the flat band potential and the number of ionized donors from

$$N_{ss}{}^2 = \frac{\varepsilon_0 \varepsilon_{sc} n_0 \varphi_0}{e} \tag{5}$$

At 20°C the calculations result in surface states of about 9.1×10^{16} [m^{-2}] for the $LaNiO_3$/PTCR interface and about 1.4×10^{17} [m^{-2}] surface states for the Ag/PTCR interface.

5. Summary

CSD turned out to be a suitable method for preparing $LaNiO_3$ thin films on polycrystalline substrates especially because of the very small grain size of the particles of the $LaNiO_3$ thin film, which enabled the growth of dense and adhesive films on the considerably rough surface of the polycrystalline substrates.

The electrical behavior of the $LaNiO_3$/PTCR-interface can be explained by the formation of a barrier layer between the n-conducting PTCR ceramic and the metallic conductor $LaNiO_3$. The barrier layer consists of a depletion layer within the PTCR ceramic and of a thin insulating layer between the $LaNiO_3$ and the PTCR ceramic. At low voltages the behavior of the insulating layer can be characterized by assuming a plate capacitor. Towards higher voltages electrons start tunneling through the insulating layer, thereby reducing the resistivity of the insulating layer. For potentials exceeding the flat band potential, the additional formation of a depletion layer within the PTCR ceramic has to be taken into account. The behavior of the depletion layer can be explained by the Mott-Schottky theory.

The characteristics of the barrier layer is qualitatively the same for $LaNiO_3$ and Ag as electrode material. The different values of the flat band potentials and the depth of the depletion layers demonstrate that $LaNiO_3$ possesses superior qualities as electrode material compared to Ag. Nevertheless, for its actual application it will be necessary to overcome the formation of insulating layers between the PTCR-ceramic and the $LaNiO_3$ electrode.

Nothing is known so far about the composition of the insulating layer. Its formation is assumed to be the result of chemical reactions taking place at the surfaces of the PTCR ceramic or the $LaNiO_3$-film during its deposition. This may be due to enhanced grain boundary oxidation of the PTCR-ceramic or to diffusion of Ni into the boundary region of the PTCR-ceramic and $LaNiO_3$ resulting in a layer of acceptor doped PTCR ceramic with high resistivities [28]. Alternatively, a transfer of electrons from the donor doped PTCR to the $LaNiO_3$ may result in the reduction of Ni^{3+} in the $LaNiO_3$ layer and a partial destruction of the perovskite structure.

Acknowledgments

We wish to thank Siemens + Matsushita Components for providing the PTCR ceramic pellets and Dr. Pölt from the Forschungsinstitut für Elektronenmikroskopie, Technische Universität Graz for the SEM investigations.

Furthermore we are grateful to Gwent Electronic Materials, UK, providing the AgZn-paste.

This work was supported by the Austrian Science Foundation (FWF) within the Special Research Program ''Electroactive Materials'' (project F 009).

References

1. H. Landolt and R. Börnstein, *Numerical Data and Functional Relationships in Science and Technology, Group 3, Volume 12, Part A: Garnets and Perovskites* (Springer, Berlin, 1978).
2. R.J.H. Voorhoeve, D.W. Johnson, J.P. Remeika, and P.K. Gallagher, *Science*, **195**, 827 (1977).
3. G. Mader, H. Meixner, and P. Kleinschmidt, *Siemens Forsch.-u. Entwickl.-Ber.*, **16**, 76 (1987).
4. W. Heywang, *Solid State Electronics*, **3**, 51 (1961).
5. S.B. Desu and D.A. Payne, *J. Am. Ceram. Soc.*, **73**(11), 3398 (1990).
6. E.J. Opila, G. Pfundtner, J. Maier, H.L. Tuller, and B.J. Wuensch, in *Proceedings of Symposium A2 on Solid State Ionics of ICAM 91*, edited by M. Balkanski, T. Takahashi and H.L. Tuller (North-Holland Elsevier Science Publishers B.V., Amsterdam, 1992).
7. N. Katsarakis, O. Fruhwirth, and W. Sitte, in *Proceedings of 4th Euroceramics*, **5**, edited by G. Gusmano and E. Traversa (Gruppo Editoriale Faenza Editrice, Faenza, 1995), p. 89.
8. P. Shuk, A. Vecher, V. Kharton, L. Tichonova, H.D. Wiemhöfer, U. Guth, and W. Göpel, *Sensors and Actuators B*, **15–16**, 401 (1993).
9. O. Fruhwirth, A. Macher, and K. Reichmann, Investigation of Electrical Behavior of $LaNi_{0.6}Co_{0.4}O_3$ on Perovskitic NTC-Ceramics, *Key Engineering Materials*, **132–136**, 1345 (1997).
10. A. Li, C. Ge, P. Lü, and N. Ming, *Appl. Phys. Lett.*, **69**(2), 161 (1996).
11. M.S. Hedge, K.M. Satyalakshmi, R.M. Mallya, M. Rajeswari, and H. Zhang, *J. Mater. Res.*, **9**(4), 898 (1994).
12. E.L. Brosha, B.W. Chung, F.H. Garzon, I.D. Raistrick, R.J. Houlton, and M.E. Hawley, *J. Electrochem. Soc.*, **142**(5), 1702 (1995).
13. D.M. Tahan, A. Safari, and L.C. Klein, *J. Am. Ceram. Soc.*, **79**(6), 1593 (1996).
14. J. Livage, M. Henry, and C. Sanchez, *Progr. Sol. State Chem.*, **18**(4), 259 (1988).
15. M. Klee, in *Proceedings of Electroceramics IV*, edited by R. Waser (Augustinus Buchhandlung, Aachen, 1994), p. 1225.
16. K.P. Rajeev, G.V. Shivashankar, and A.K. Raychaudhuri, *Sol. Stat. Commun.*, **79**(7), 591 (1991).
17. K. Sreedhar, J.M. Honig, M. Darwin, M. McElfresh, P.M. Shand, J. Xu, B.C. Crooker, and J. Spalek, *Phys. Rev. B*, **46**(10), 6382 (1992).
18. P. Ganguly and C.N.R. Rao, *Mat. Res. Bull.*, **8**, 405 (1973).
19. P. Ganguly, N.Y. Vasanthacharya, C.N.R. Rao, and P.P. Edwards, *J. Solid State Chem.*, **54**, 400 (1984).
20. J. Drennan, C.P. Tavares, and B.C.H. Steele, *Mat. Res. Bull.*, **17**, 621 (1982).
21. A. Li, C. Ge, P. Lü, and N. Ming, *Appl. Phys. Lett.*, **68**(10), 1347 (1996).
22. D.Y. Wang and K. Umeya, *J. Am. Ceram. Soc.*, **74**(2), 280 (1991).
23. J. Daniels, K.H. Härdtl, and R. Wernicke, *Philips techn. Rdsch.*, **38**(1), 1 (1979).

24. S.M. Sze, *Physics of Semiconductor Devices,* 2nd Edition (John Wiley and Sons, New York, 1981).
25. J.F. Dewald, *J. Phys. Chem. Solids*, **14**, 155 (1960).
26. Y.Y. Lu, C.H. Lai, and T.Y. Tseng, *J. Am. Ceram. Soc*., **77**(9), 2461 (1994).
27. M.S. Correia and J.L. Baptista, in *Ceramics Today—Tomorrow's Ceramics*, edited by P. Vincenzini (Elsevier Science Publishers, Amsterdam, 1991), p. 2073.
28. S.B. Desu and D.A. Payne, *J. Am. Ceram. Soc*., **73**(11), 3416 (1990).